Journal of Engineering and Technology for Industrial Applications

ITEGAM-JETIA

Manaus, v.12 n.58, p.844-854 March/April, 2026.
DOI: https://doi.org/10.5935/jetia.v12i58.3104

ISSN ONLINE: 2447-0228

RESEARCH ARTICLE OPEN ACCESS

EMBRYO SELECTION AND CLASSIFICATION IN IVF USING HYBRID DEEP LEARNING APPROACH

J. Deepa[*1] and A. Akila[2]

[1]Research Scholar, Department of Computer Science, School of Computing Sciences,Vels Institute of Science, Technology and Advanced Studies (VISTAS), Chennai, India.
[2]Associate Professor, Department of Computer Science, School of Computing Sciences, Vels Institute of Science, Technology Advanced Studies (VISTAS), Chennai, India.

[1]http://orcid.org/0009-0007-2227-9291, [2]http://orcid.org/0000-0001-7744-3473

Email: *pushdeepa3@gmail.com, akila.scs@vistas.ac.in

ARTICLE INFO

Article History
Received: December 11, 2025
Reviewed: January 14, 2026
Accepted: March 10, 2026
Published: April 30, 2026

Keywords:
IVF
embryo selection
CLAHE
SSS-Net
CNN-LSTM

ABSTRACT

Accurately evaluating and choosing viable embryos for implantation is crucial to the success rate of in vitro fertilisation (IVF). Traditional evaluation techniques mostly rely on the subjective and variable eye observation of embryologists. This study suggests a deep learning-based automated embryo classification framework that combines image preprocessing, segmentation, and classification in order to overcome these drawbacks. First, to improve the contrast and clarity of small morphological characteristics in embryo photos, Contrast Limited Adaptive Histogram Equalisation (CLAHE) is used. The enhanced images are then subjected to a sprint semantic segmentation network (SSS-Net) to ensure that only relevant features support classification and accurately differentiate the embryo region from the backdrop. Using a hybrid Convolutional Neural Network–Long Short-Term Memory (CNN–LSTM) model, the last step successfully classifies embryos into different quality categories. This method captures both spatial and sequential feature dependency. The experimental evaluation demonstrates the durability and dependability of the proposed framework with high precision, recall, F1-score, and accuracy, demonstrating strong predictive performance. When compared to conventional techniques, the combination of sophisticated preprocessing, effective segmentation, and hybrid deep learning architecture greatly increases classification consistency. All things considered, the suggested method offers an automated, scalable, and objective tool for evaluating the quality of embryos. It may also help embryologists make clinical decisions and eventually increase the success rates of IVF.

I. INTRODUCTION

About 80 million couples worldwide suffer from infertility, a serious issue and major clinical condition that affects 8–12% of couples [1]. Globally, the infertility rate has been steadily rising, and in many West African groups, it is even getting close to 50% [2]. According to estimates, only half of the 6.1 million infertile Americans receiving therapy are receiving fertility-related care [3]. One popular and successful assisted reproductive method for treating infertility is in vitro fertilisation (IVF). Using a manual fertilisation process, IVF involves cultivating embryos in an incubator for three to five days until they reach the blastocyst stage.

Based on important morphological characteristics, the best embryos (blastocysts) are chosen and returned to the patient's uterus [4]. To boost the likelihood of pregnancy, several blastocysts were transferred in the past. But it caused mothers and newborns to have repeated pregnancies and other gestational problems. In order to lower the chance of multiple pregnancies, it is advised to transfer a single viable blastocyst [5]. In the past, skilled embryologists have closely examined the morphological features of blastocyst components using time-lapse imaging to physically assess the embryo's viability.

Pregnancy is significantly impacted by the various morphologies of the blastocoel (BL), inner cell mass (ICM), trophectoderm (TE), and zona pellucida (ZP), which are the fundamental components of the blastocyst [6]. Sperm-egg binding depends on ZP, a protective glycoprotein coating that envelops the oocyte. ZP thickness reduces when the embryo moves on to the blastocyst stage and is highly correlated with IVF success. A layer of cells called TE is necessary for the production of the fluid that makes up the placenta. There is a substantial correlation between embryo viability and TE morphology and quality [7]. Because the survival and potential of the subject embryo depend on the features of its component parts taken together, the morphometric evaluation of the blastocyst is a crucial goal for an embryologist [8].

I.1 OBJECTIVES

- To design and implement a fully automated system that objectively classifies embryo images, reducing dependence on manual visual inspection by embryologists.
- • To use Contrast Limited Adaptive Histogram Equalisation (CLAHE) to emphasise fine morphological details that are essential for precise analysis and to improve image contrast.
- To employ a Sprint Semantic Segmentation Network (SSS-Net) for precise embryo delineation, ensuring that only relevant morphological features are analyzed.
- To develop a hybrid CNN–LSTM model that effectively integrates spatial (from CNN) and temporal or sequential (from LSTM) information for robust embryo quality classification.

I.2 CONTRIBUTIONS

- The study minimises human subjectivity and inter-observer variability in traditional evaluation methods by introducing a fully automated deep learning-based system for assessing embryo quality.
- By enhancing the visibility of subtle structural elements in embryo photos, Contrast Limited Adaptive Histogram Equalisation (CLAHE) makes it easier to segment and classify images later on.
- The embryo zone is precisely separated from the backdrop using a specialised segmentation network called SSS-Net, guaranteeing that classification models only concentrate on biologically significant features.
- More robust classification performance is achieved by the suggested hybrid CNN–LSTM model, which incorporates both temporal (developmental) dependencies and spatial patterns in embryo morphology.
- The framework has been thoroughly tested using a variety of performance metrics, including precision, accuracy, recall, and F1-score, and shows better predicted reliability and consistency than conventional visual assessment techniques.

Section 2-Related Work: This part examines the body of research on methods for evaluating the quality of embryos, with an emphasis on both current developments in deep learning-based image analysis and more conventional visual evaluation techniques. Section 3: Methodology: This section provides a detailed description of the suggested automated embryo classification framework, including the use of CLAHE for picture preprocessing, the Sprint Semantic Segmentation Network (SSS-Net) for embryo segmentation, and the hybrid CNN–LSTM architecture for classification. Section 4: Findings and Analysis The experimental findings are shown and discussed in this section, along with a comparison of the suggested framework's accuracy, precision, recall, and F1-score with baseline and conventional approaches. Section 5-Conclusion: This section outlines the study's practical implications for clinical IVF applications, highlights the key findings, and makes recommendations for possible future research routes.

II. RELATED WORK

The research article [9] that conducted a multicenter randomised clinical experiment comparing traditional morphological evaluation of embryos in IVF with deep learning (iDA Score). Given that the clinical pregnancy rate was 48.2% based on morphology and 46.5% based on iDA Score, deep learning did not demonstrate noninferiority (risk difference -1.7; 95% CI -7.7, 4.3; P=0.62). The paper [10] a study that improved the embryo selection during IVF by developing a deep learning algorithm based on time-lapse imagery and self-supervised contrastive learning.

With an AUC of 0.57 based on prior transfer knowledge and 0.64 without it, the algorithm, which was trained on 1,580 videos of 460 patients' embryos, predicted the success of implantation. The experiment [11] that developed and evaluated machine learning models to forecast blastocyst incidence during IVF cycles. With fewer characteristics and better interpretability than SVM and XGBoost, LightGBM was the best. The percentage of 8-cell embryos and long culture embryos, as well as the number of cells on Day 3, were significant predictors. The article under review [12] which compared the application of an AI platform to support FSH dosing and timing of trigger stimulation in IVF among 291 patients.

AI assisted treatment demonstrated a slightly greater MII oocytes count, total oocytes recovered, and FSH consumption which indicated that AI could be used safely to maximize ovarian stimulation. The study [13] in which the authors proposed IVFormer with VTCLR, an AI that predicts the embryo status and live-birth rates using multi-modal and unlabelled data. The algorithm outperformed the physicians in the euploidy ranking, suggesting that it could be a non-invasive and reasonably priced way to choose embryos. The study [14] that looked at the effects of adding 15% additional training data to iDAScore v2.0, a technique used to predict sustained pregnancy following single vitrified warmed blastocyst transfer (SVBT).

With over 15% of training data, iDAScore v2.0 outperformed iDAScore v1.0 or Gardner grading in predicting ongoing pregnancy (iDAScore v2.0 AUC scores 0.736 vs. 0.720 vs.The article [15] that has developed a Convolutional LSTM-based artificial intelligence system that can analyse the last two hours to anticipate the morphology of embryos up to 23 hours in advance. In order to facilitate early and non-invasive embryo selection, the system separated transferable embryos from those that should be avoided. The research [16] which created DeepEmbryo a machine learning-powered device that can predict the success of the pregnancy based on three time-lapse images of the embryo.

DeepEmbryo was able to outperform algorithms that only used the final image and outperformed five trained embryologists, with as high as 75% accuracy. The study [17] under consideration at the possibility of AI involvement into the surgical decision-making process, but patient safety, ethics, transparency, interpretability, and collaborative work on responsible AI application in healthcare are the key concerns. The article [18] which comprises a review of the microfluidics in sperm selection of IVF and ICSI. Microchannel chips are able to sort highly motile sperm with low impacts and DNA damage, enhancing success rates, yet commercialization and species applications are problematic.

It is the study [19] where the models of MLCS live birth prediction were compared to the national registry of SART. MLCS was superior to SART in the recognition of patients with better live birth chances and it has potential in personalized counseling and clinical decision making. The study [20] that trained a hybrid AI model with day-5 images of the blastocysts and clinical and laboratory data to determine the chances of implantation. Heatmaps have been used to reveal inner cell mass, trophectoderm and blastocyst growth and have been shown to be useful in interpretable embryo level decisions. The article [21] who created three AI models, including clinically-based MLP, image-based CNN, and a combination of the two to forecast clinical pregnancy and live birth in single embryo transfer.

The accuracy of the fusion model was 82.42 and AUC was 0.91. The research under consideration [22] that constructed an AI system by applying Attention Branch Networks to predict live birth based on 141,444 embryo images of 470 transfers. Embryos with a score of more than 0.341 showed much better live births, which argue in favor of non-invasive selection. This study [23] systematic review of CNN models to assess embryos through time-lapse monitoring in 22 retrospective studies using 522,516 images of 222,998 embryos. CNNs also performed better than embryologists, particularly in the classification of blastocyst stage.

The corresponding article [24] which is a review of AI usage in embryo grading and pregnancy prediction based on multi-modal data. There are data scarcity, multi-modal features combination, and generalization of models. It is [25], which described an AI system based on Convolutional LSTM that predicts embryo morphology and separates transferable embryos, helping to select embryos early on in a non-invasive procedure. The research [26] where five ML models have been compared in relation to the use of GA feature selection in predicting IVF outcomes. AdaBoost using GA had an 89.8% accuracy and female age, AMH, endometrial thickness, sperm count and embryo quality were found to be significant predictors.

The study [27] that produced ML models that predicted the outcomes of live births of 11,938 Chinese IVF couples. Best were logistic regression and Random Forest (AUROC of~0.67), where maternal age, progesterone and estradiol made the greatest contributions. The resemblant article [28] an overview of AI in ART labs, which includes data gathering, record keeping, embryo selection, and automation to decrease subjectivity and human error. The corresponding research article [29] which reported the use of AI software in ART to facilitate IVF processes, minimize interobserver discrepancy, discover how to optimize drug dosing and enhance gamete quality. Closely connected is the review article [30] that examined the current state of ML to determine the quality of sperms and oocytes, and emphasised its value in the accurate assessment of the gametes and the possible increase in the ART success.

The researchers [31] who have suggested hill-climbing feature selection based on ML models as predictors of IVF pregnancy success. Significant variables were age, AFC, number of MII, and embryo transfer day that enhanced prediction. The article [32] which compared ML (SVM and neural networks) and logistic regression in terms of IVF outcomes. ML was superior to logistic regression in terms of the number of oocytes recovered, embryo quality, clinical pregnancies and live births. The work [33] that developed machine learning algorithms to calculate the optimal number of embryos to transfer in order to maximise the transfer rate. SVM and ANN achieved the best accuracy (95.83% and 91.67), suggesting the potential for individual embryo-transfer decisions. The corresponding article [34] a review of deep learning to automatically grade IVF blastocysts.

Automated techniques can usually be as good or better than embryologist performance. The paper [35] which introduced a two-stage deep learning method of automatic tracking of follicular growth with SFR-Net based on 3D UNet and Multi-Scale Residual Blocks with a DICE score of 85.84. It is related to [36] reviewing AI in ART, which includes image analysis, personalised protocols, and workflow automation, with ethical, regulatory, and sustainability issues being addressed. The experiment is [37] where the authors used end-to-end deep learning to infer embryo ploidy using 690 raw time-lapse videos on their dataset and achieved a baseline AUC 0.74, showing evidence of the ploidy assessment can be non-invasive. The corresponding piece [38] which reviews AI based automated embryo assessment at different stages of development, which is associated with higher selection efficiency, enhanced performance over manual assessment, limitations and future research priorities.

III. PROPOSED METHODOLOGY

The proposed approach offers a deep learning-based pipeline for automated embryo categorisation in in vitro fertilisation (IVF) to improve the accuracy and objectivity of assessing the quality of embryos. The framework's three primary stages are preprocessing, classification, and segmentation. CLAHE is used during the preprocessing phase to improve the contrast and brightness of embryo images. This makes it easier to see minute morphological details that are necessary for precise analysis. To make sure that only pertinent characteristics are used in following phases, the improved images are subsequently run through a SSS-Net, which successfully separates the embryo region from the surrounding background and artefacts

A hybrid CNN–LSTM model is employed for the classification stage. The CNN component extracts deep spatial information to improve the model's capacity to identify developmental trends in various embryo pictures, while the LSTM component records temporal and sequential correlations. The suggested method yields performance metrics with exceptional resilience and dependability, including as accuracy, precision, recall, and F1-score. This integrated approach reduces human subjectivity and promotes better clinical judgement during IVF procedures by providing a strong tool for automated evaluation of embryo quality.

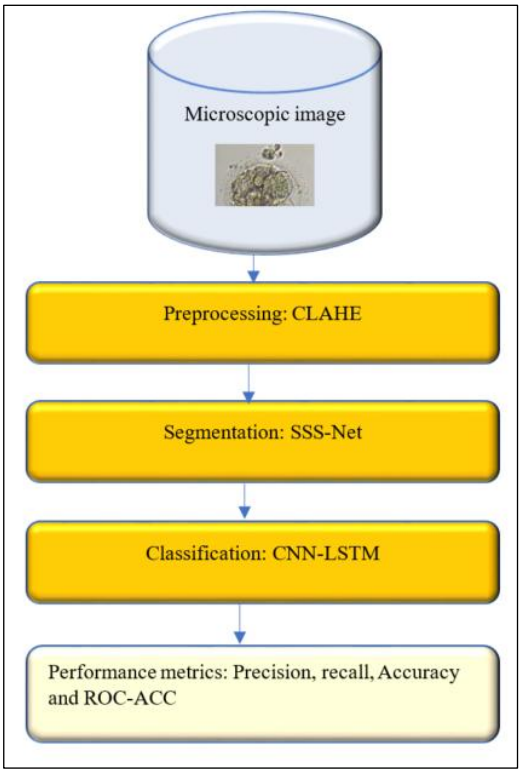

Figure 1: Flow diagram of proposed embryo selection.
Source: Authors, (2026).

III.1 DATASET: EMBRYO CLASSIFICATION BASED ON MICROSCOPIC IMAGES

The embryo images are arranged within subfolders under the train and test directories. Each image is saved in JPG format and is labelled with a prefix. Images corresponding to day-3 embryos have the prefix D3 while images related to day-5 embryos bear the prefix D5. This prefix-based categorization allows for easy identification of the embryo's developmental stage.

III.2 PREPROCESSING: CLAHE (CONTRAST-LIMITED ADAPTIVE HISTOGRAM EQUALIZATION)

Adaptive Histogram with Contrast Limitations An image processing technique called equalisation is used to increase an image's contrast. Instead of using a complete image, CLAHE works in a tile call, which is a small portion of an image. The histogram's use is distinct from its general use, where each tile is changed by calculating the function of the condition of being contrasted colour. The distributed value for each tile contrast is added to the histogram of the resolution region approximation to it. The adjacent tiles then joined to prevent induced borders. To prevent enhancing any potential noise in the image, the contrast will be kept to a minimum, mostly in areas that are uniform. The image x has greyscale equalisation in the Histogram, and the value is greyscale up to 256. In contrast, the following formula should be used to find the probabilities at pixel level I in an image:

$$D_x(i) = D_{(x=i)} = \frac{n_i}{n}, 0 \leq i < L \quad (1)$$

In this case, the variable L denotes the image's overall grey level count, which is typically 256, and the variable n denotes the dataset's pixel count. The image histogram for the pixel into an index to i is represented by the variable $D_x(i)$.

III.3 SEGMENTATION: SPRINT SEMANTIC SEGMENTATION NETWORK (SSS-NET)

In order to precisely identify and characterise important blastocyst components, this work presents a lightweight semantic segmentation framework for embryological investigation. By avoiding computationally costly preprocessing methods, the suggested SSS-Net enhances image contrast without sacrificing speed. Instead, it uses skip connection blocks (SCBs) in the encoder to directly handle the raw input images and recover biassed and rich feature representations. By using a shallow upsampling block, the decoder effectively and simply reconstructs spatial features.

SSS-Net produces a five-channel segmentation mask at the output, with each channel representing a different class: background, blastocoel (BL), trophectoderm (TE), zona pellucida (ZP), and inner cell mass (ICM). By assigning a value of "1" to each component pixel and a "0" to non-component regions, these masks enable accurate morphological evaluation of every blastocyst structure. By enabling the objective evaluation of blastocyst morphology, this segmentation aids in the precise determination of embryo viability.

Encoder Block

Since the decoder's complexity equals that of the encoder, conventional semantic segmentation systems usually employ identical encoder and decoder architectures, significantly increasing the number of trainable parameters.

On the other hand, the suggested SSS-Net minimises model complexity and computational cost by introducing a shallow semantic segmentation architecture with a lightweight upsampling module that employs a small number of transposed convolution layers. Figure 2 depicts the SSS-Net layer-by-layer design. The network uses three stride convolutions rather than several pooling layers to gradually shrink the feature map size while retaining learnable weights in order to protect important spatial information and prevent excessive feature loss. Additionally, by lowering feature transfer impedance issues that are commonly observed in conventional architectures, dense connections are utilised to offer efficient feature propagation between layers.

Within each Skip Connection Block (SCB), a point-wise convolution $\text{Conv}_{1,1}$ receives the input feature I_i from the Rectified Linear Unit (ReLU) activation of the preceding SCB, while a separable convolution Conv_{Sep} processes the same I_i in parallel. The resulting point-wise features G_i from $\text{Conv}_{1,1}$ are simultaneously fed into two asymmetric kernel-based convolutions $\text{Conv}_{1,3}$ and $\text{Conv}_{3,1}$ and one standard convolution $\text{Conv}_{3,3}$, producing feature maps K_{A_i}, K_{B_i}, and L_i, respectively. The outputs from the asymmetric convolutions, K_{A_i} and K_{B_i}, are concatenated to form D_{A_i}, as defined in Equation (2). After Batch Normalization (BN) and ReLU activation, this combined feature becomes D'_{A_i}, which is subsequently utilized for further feature fusion and representation learning.

$$D_{Ai} = K_i^A © K_i^B \tag{2}$$

The depth-wise concatenation between the features K_{A_i} and K_{B_i} is represented by the symbol ©. After the Batch Normalization (BN) and Rectified Linear Unit (ReLU) operations, the features F_i and L_i, generated by Conv_{Sep} and $\text{Conv}_{3,3}$, respectively, are transformed into F'_i and L'_i. The enhanced feature D_{B_i}, as expressed in Equation (3), is obtained by combining the asymmetric convolution feature D'_{A_i} with the outputs F'_i and L'_i from Conv_{Sep} and $\text{Conv}_{3,3}$. The spatial information from F'_i, imported from the preceding block, contributes to the refinement of the D_{B_i} feature representation. At the end of the SCB, a bottleneck point-wise convolution $\text{Conv}_{1,1}$, followed by Batch Normalization (BN), is applied to D_{B_i}, producing the final feature map D'_{B_i}. The activation function utilized in this stage, ReLU, is defined by Equation (4).

$$D_{Bi} = D'_{Ai} © L'_i © F'_i \tag{3}$$

$$D_{Bi}{}' = [D'_{Ai} © L'_i © F'_i]' \tag{4}$$

The depth-wise concatenation of features D′Ai, L′i, and F′i is displayed here by ©. The next SCB will have Feature D′Bi, the last feature from the suggested SCB that combines three distinct features. Unlike conventional semantic segmentation designs, SSS-Net has a unique shallow decoder block that uses only three transposed convolutional layers for upsampling. The feature map DBi', DBi ′undergoes three consecutive dimensional reductions twice in the final skip connection block (SCB), and the feature map is upsampled three times using these transposed convolutions to restore the original input dimensions. The shallow decoder architecture reduces computational complexity by using fewer layers for upsampling while maintaining effective feature reconstruction.

To improve deep feature learning, the decoder combines four convolutional layers that reduce the semantic gap between the decoder and the transposed convolutional layers. Three transposed convolutions gradually upscale the feature maps to the original resolution, providing detailed spatial information to the final pixel classification block. The pixel classification layer uses a Tversky loss function to reduce class disparity and improve segmentation performance. This layer consists of a curve function with filters corresponding to the number of target classes. The Tversky loss (TLoss) is mathematically defined in Equation (5).

$$T_{Loss} = \frac{\sum_{i=1}^{N} P_b^i G_b^i + \omega}{\sum_{i=1}^{N} P_b^i G_b^i + \omega + \alpha \sum_{i=1}^{N} P_b^i G_b^i + \beta \sum_{i=1}^{N} P_b^i G_{nb}^i + \omega} \tag{5}$$

Where Pib and Gib, respectively, represent the likelihood that a pixel is part of the blastocyst and non-blastocyst components. A blastocyst and a non-blastocyst component are reflected in the gib and ginb pixels of the ground truth, respectively.

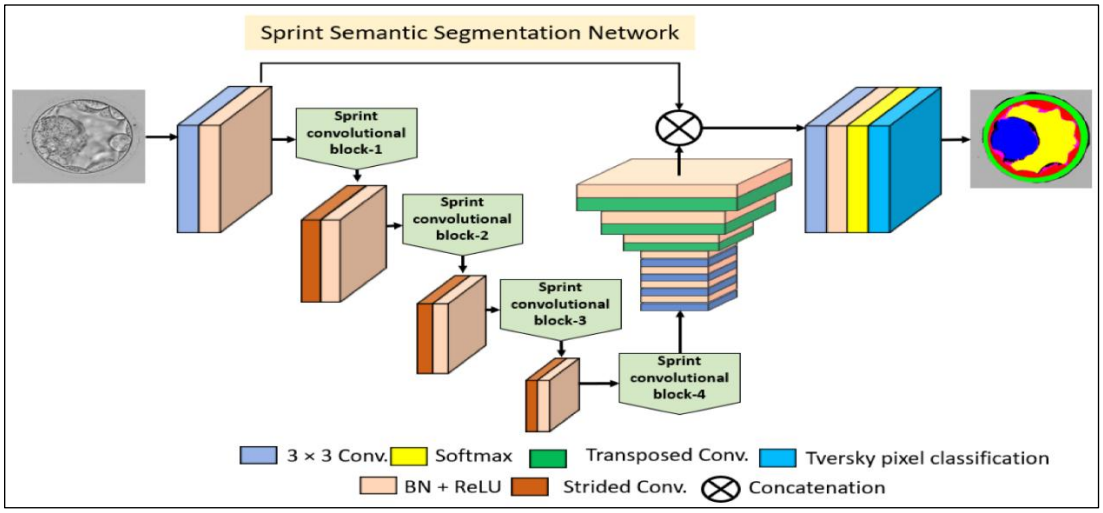

Figure 2: Architecture of SSS-Net.
Source: Authors, (2026).

III.4 CLASSIFICATION: CNN-LSTM

An activation value is produced by convolutional neural networks, or CNNs, after the different inputs are computed using mathematical functions. Artificial neurones are similar to the neurones in the human brain, which receive and process a wide range of input signals and responses. CNN is composed of several layers of artificial neurones and processes the images using a powerful algorithm. Complex objects and patterns can be learnt by convolutional neural networks (CNNs). They are made up of millions of parameters, several hidden layers, an input layer, and an output layer. The three layers that make up CNN are convolutional, pooling, and fully connected (FC). Using the output from the previous layer, the following layer pulls features from the photos, such as edges and corners. The first layer that is utilized to extract features from images is the convolutional layer.

The Convolved Feature's size is decreased by the second Pooling layer. To link neurons between two layers, weight and bias are applied to the neurons in the completely connected layer. When all features are added to the fully connected layer during the dataset training phase, overfitting takes place. By excluding a small number of neurons during training, a dropout layer shrinks the model's size and boosts performance. The model can be trained faster and achieve better results by using the rectified linear activation function. It is a linear function that will immediately output the input if the value of t is positive; else, it will output zero. As the last layer's final output and activation layer, Soft-max functions as a multiclassifier.

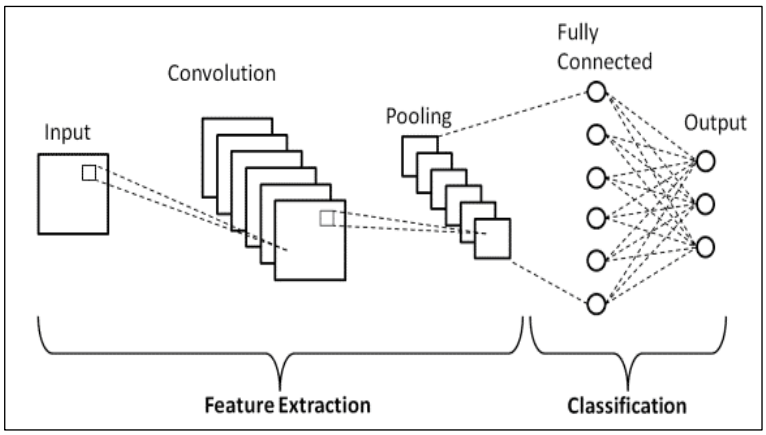

Figure 3: Architecture of CNN.
Source: Authors, (2026).

III.5 LSTM (LONG SHORT-TERM MEMORY)

The LSTM network's distinct memory cell layout enables it to disseminate and store data across multiple time steps. The cell state is the main component that stores temporal information and allows the network to recognise dependencies in sequential data. Three distinct gate types input, output, and forget gates are combined in the LSTM architecture to guarantee efficient learning of long-term dependencies. Together, these gates regulate how information enters, moves through, and exits the cell. Time-series meteorological data was used to train LSTM-based neural networks to predict the stages of embryo selection. The model's ability to effectively handle temporal patterns was utilised in this investigation. The organisation of the LSTM architecture is depicted in Figure 4.

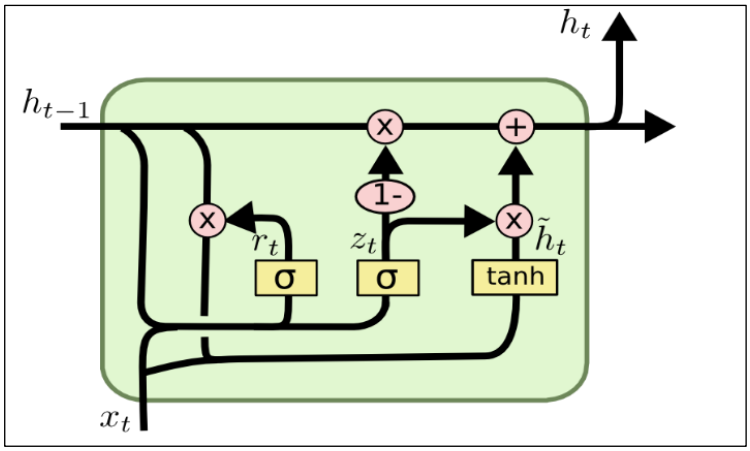

Figure 4: Structure of LSTM.
Source: Authors, (2026).

Because LSTM gates are sigmoid activation functions, they often yield a value between 0 and 1. The input, forgotten, and output gates' mathematical expressions are as follows.

$$i_t = \sigma(w_i[h_{t-1}, x_t] + b_i) \tag{6}$$

$$f_t = \sigma(w_f[h_{t-1}, x_t] + b_f) \tag{7}$$

$$o_t = \sigma(w_o[h_{t-1}, x_t] + b_o) \quad (8)$$

$i_t, f_t \, and \, o_t - Input \, gate, forget \, gate \, and \, output \, gate,$
$\sigma - sigmoid \, function,$
$w_x - weight \, for \, input, forget \, gate \, and \, output \,,$
$h_{t-1} - previous \, the \, LSTM \, block \, at \, the \, time \, (t-1),$
$x_t - time \, slot \, at \, icurrent \, nput \,,$
$b_x - biases \;\; for \, input, forget \, gate \, and \, output \, gate.$

The output equations for the cell state, candidate state, and final state are expressed as follows:

$$\tilde{C}_t = \tanh\,(w_c[h_{t-1}, x_t] + b_c) \quad (9)$$

$$C_t = f_t * C_{t-1} + i_t * \tilde{C}_t \quad (10)$$

$$h_t = o_t * \tanh\,(C^t) \quad (11)$$

Whereas,
$C_t - cell \, state,$
$\tilde{C}_t - candidate \, for \, cell \, state \, timeslot(t).$

IV. RESULT AND DISCUSSION

The proposed embryo classification framework was evaluated using a dataset of annotated embryo images collected from IVF procedures. Standard assessment measures, such as accuracy, precision, recall, and F1-score, were used to evaluate the system's performance. After applying CLAHE preprocessing, a significant improvement in image clarity and contrast was observed, enhancing the visibility of key morphological structures. The SSS-Net segmentation model effectively extracted embryo regions, achieving precise boundary delineation and minimizing background noise, which improved the quality of input data for classification. The process is implemented in python language and google colab tool.

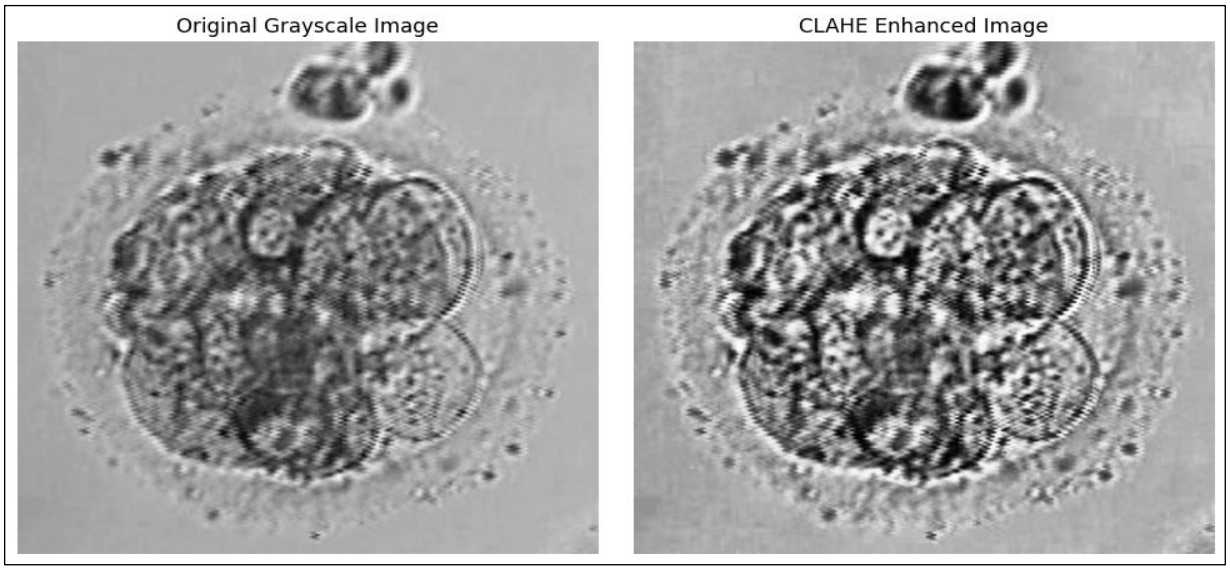

Figure 5: Preprocessed image.
Source: Authors, (2026).

The effect of CLAHE enhancement is illustrated in Figure 5, which compares the original grayscale embryo image with the contrast-enhanced version. As shown, CLAHE effectively increases the visibility of subtle embryo structures without introducing excessive noise, thereby improving the quality of data fed into the deep learning models for segmentation and classification

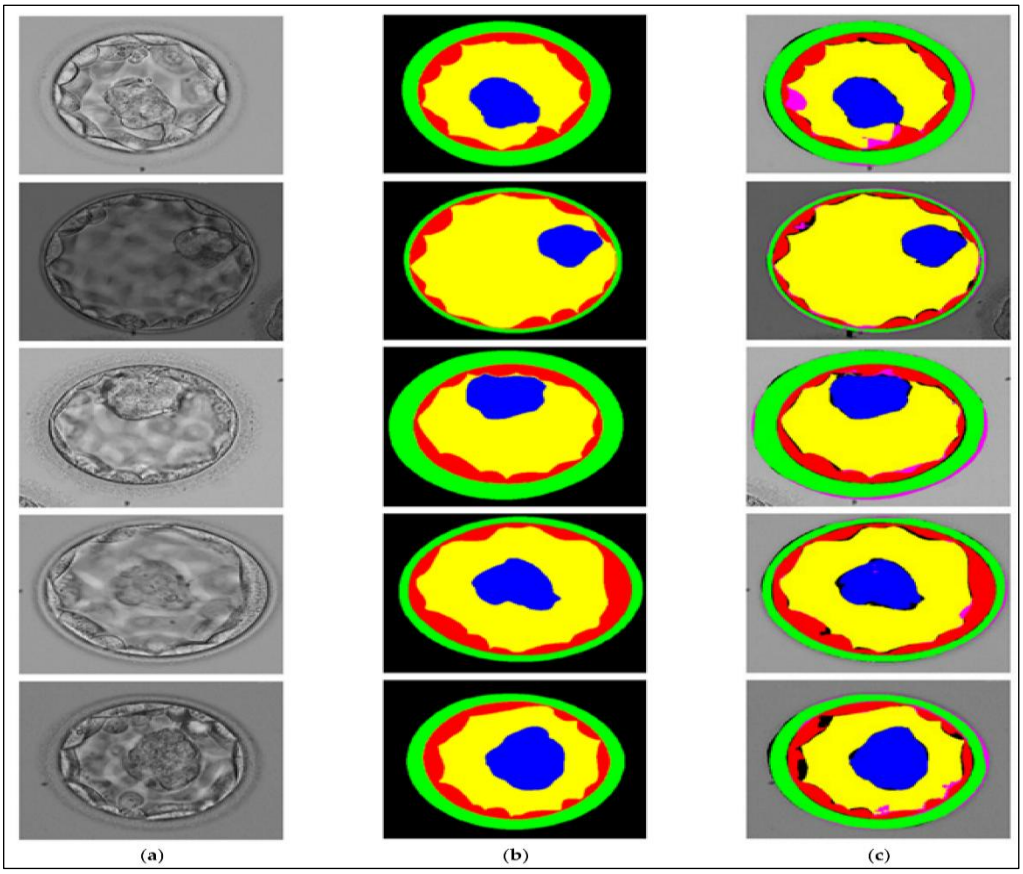

Figure 6: SS-Net for blastocyst component detection
Source: Authors, (2026).

Figure 6 displays the visual outcomes of blastocyst image segmentation utilising the suggested SSS-Net and the related ground truth (GT) images. The colours green, red, yellow, blue, and black/no (for GT/predicted) stand for the classes ZP, TE, BL, and ICM, respectively. The predicted image's pink hue indicates false negatives, or areas where the model was unable to detect a structure in the ground truth, with the GT = 1 and the anticipated mask = 0. On the other hand, false positive pixels areas that are mistakenly identified as belonging to a structure are displayed in black within the anticipated image when predicted mask = 1 and GT = 0.

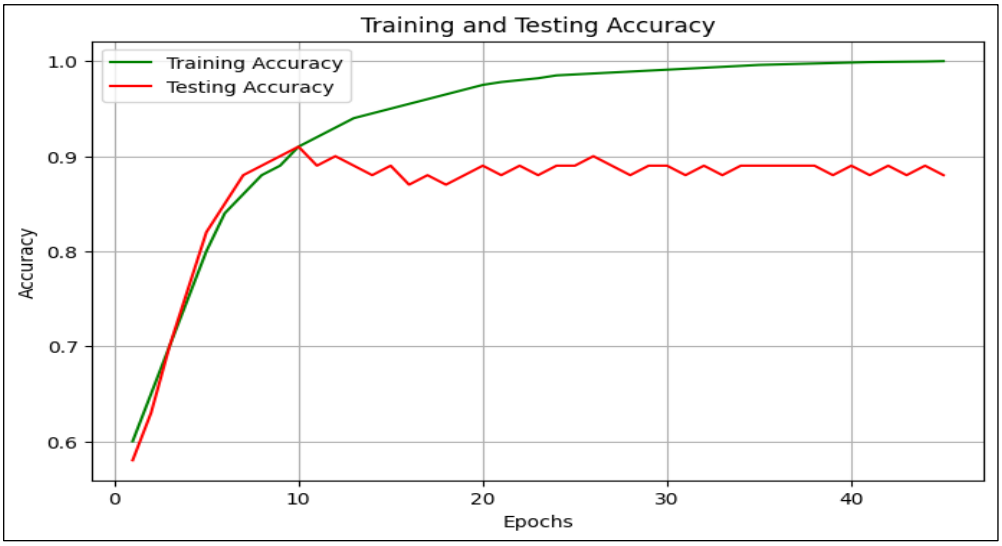

Figure 7: Training and testing accuracy.
Source: Authors, (2026).

Figure 7, which displays the training and testing accuracy curves over all epochs, shows how well the suggested model performed during the training phase. During training, the model consistently improves its accuracy, reaching convergence after about 40 epochs. The testing accuracy follows a similar trend and stabilizes early, indicating that the model effectively learns discriminative embryo features without significant overfitting. The close alignment between the two curves suggests that the hybrid CNN–LSTM architecture successfully generalizes across unseen data, confirming the robustness of the proposed approach for automated embryo classification.

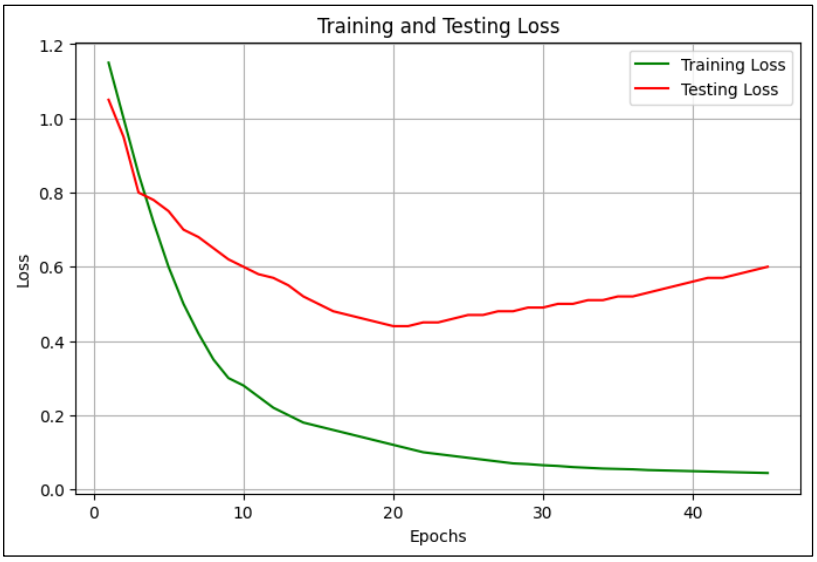

Figure 8: Training and testing loss.
Source: Authors, (2026).

The training and testing loss curves of the proposed model are presented in Figure 8. As shown, the training loss decreases steadily with the number of epochs, demonstrating the model's progressive improvement in minimizing classification errors. The testing loss also follows a downward trend and plateaus early, confirming that the network generalizes well to unseen data. The close correspondence between the two loss curves suggests that the model avoids overfitting and maintains strong generalization performance. These results further validate the effectiveness of the hybrid CNN–LSTM architecture in learning spatial and temporal embryo features essential for accurate classification.

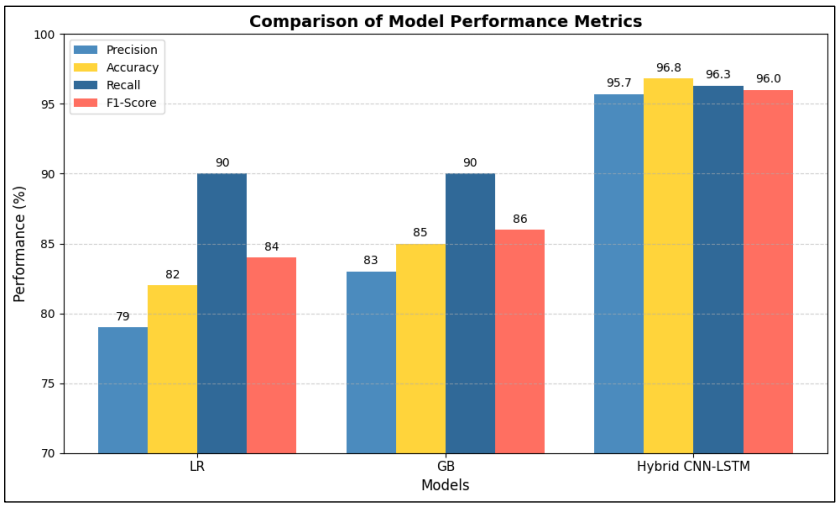

Figure 9: Comparasion model.
Source: Authors, (2026).

Figure 9 compares the performance of three models on the embryo classification dataset: Logistic Regression (LR), Gradient Boosting (GB), and the proposed Hybrid CNN–LSTM architecture. The outcomes unequivocally show that the hybrid model based on deep learning performs noticeably better than conventional machine learning techniques. With an F1-score of 96.0%, recall of 96.3%, accuracy of 96.8%, and precision of 95.7%, the Hybrid CNN–LSTM provides the best results on all performance parameters. This illustrates how well the model can categorise embryos and maintain a performance balance between sensitivity and precision. The traditional models (LR and GB), on the other hand, show a modest level of accuracy and a higher rate of misclassification, underscoring their poor capacity to capture intricate temporal and spatial embryonic aspects. These findings support the suggested hybrid deep learning model's effectiveness and resilience for accurate evaluation of embryo quality.

V. CONCLUSION

The deep learning-based system for automated embryo categorisation in IVF is presented in this paper, which combines sophisticated image preprocessing, segmentation, and classification methods. The visual clarity of embryo structures was greatly increased by using CLAHE for contrast enhancement, which made it possible to retrieve morphological details more effectively. By precisely separating embryo areas, the SSS-Net segmentation model decreased background interference and improved the dependability of the collected data. Both temporal and spatial dependencies in embryo images were well captured by the hybrid CNN–LSTM classifier, allowing for reliable and reliable classification across quality categories.

The system's ability to conduct accurate evaluations of embryo quality was confirmed by the experimental findings, which showed good F1-score of 96.0%, recall of 96.3%, accuracy of 96.8%, and precision of 95.7%, the Hybrid CNN–LSTM provides the best results on all performance parameters. The suggested approach provides increased objectivity, reproducibility, and efficiency above traditional manual examination. This strategy may prove to be a useful tool for embryologists in making decisions, helping them choose embryos and increasing the success rates of IVF. To improve model interpretability and clinical acceptability, future research might concentrate on growing the dataset size, adding multi-modal imaging data, and implementing explainable AI approaches. All things considered, the suggested approach is a major step forward for reproductive medicine's completely automated, data-driven embryo examination.

VI. AUTHOR'S CONTRIBUTION

Conceptualization: J. Deepa and A. Akila.
Methodology: J. Deepa and A. Akila.
Investigation: J. Deepa and A. Akila.
Discussion of results: J. Deepa and A. Akila.
Writing – Original Draft: J. Deepa and A. Akila.
Writing – Review and Editing: J. Deepa and A. Akila.
Resources: J. Deepa and A. Akila.
Supervision: J. Deepa and A. Akila
Approval of the final text: J. Deepa and A. Akila.

VII. REFERENCE

[1] Purkayastha, N.; Sharma, H. Prevalence and Potential Determinants of Primary Infertility in India: Evidence from Indian Demographic Health Survey. Clin. Epidemiol. Glob. Health 2021, 9, 162–170.

[2] Lepore, M.; Petruzziello, A. A Situation-Aware DSS to Support Assisted Reproductive Technology Outcome Prediction. In Proceedings of the IEEE Conference on Cognitive and Computational Aspects of Situation Management, Tallin, Estonia, 14–21 May 2021; pp. 103–107.

[3] Galic, I.; Swanson, A.; Warren, C.; Negris, O.; Bozen, A.; Brown, D.; Lawson, A.; Jain, T. Infertility in the Midwest: Perceptions and Attitudes of Current Treatment. Am. J. Obstet. Gynecol. 2021, 225, 61.e1–61.e11.

[4] Le, M.T.; Nguyen, T.T.T.; Nguyen, T.V.; Dang, H.N.T.; Nguyen, Q.H.V. Blastocyst Transfer after Extended Culture of Cryopreserved Cleavage Embryos Improves in Vitro Fertilization Cycle Outcomes. Cryobiology 2021, 100, 26–31.

[5] Li, Y.; Liu, S.; Lv, Q. Single Blastocyst Stage versus Single Cleavage Stage Embryo Transfer Following Fresh Transfer: A Systematic Review and Meta-Analysis. Eur. J. Obstet. Gynecol. Reprod. Biol. 2021, 267, 11–17.

[6] Bori, L.; Dominguez, F.; Fernandez, E.I.; Del Gallego, R.; Alegre, L.; Hickman, C.; Quiñonero, A.; Nogueira, M.F.G.; Rocha, J.C.; Meseguer, M. An Artificial Intelligence Model Based on the Proteomic Profile of Euploid Embryos and Blastocyst Morphology: A Preliminary Study. Reprod. Biomed. Online 2021, 42, 340–350.

[7] Ozgur, K.; Berkkanoglu, M.; Bulut, H.; Donmez, L.; Isikli, A.; Coetzee, K. Blastocyst Age, Expansion, Trophectoderm Morphology, and Number Cryopreserved Are Variables Predicting Clinical Implantation in Single Blastocyst Frozen Embryo Transfers in Freeze-Only-IVF. J. Assist. Reprod. Genet. 2021, 38, 1077–1087.

[8] Sciorio, R.; Meseguer, M. Focus on Time-Lapse Analysis: Blastocyst Collapse and Morphometric Assessment as New Features of Embryo Viability. Reprod. Biomed. Online 2021, 43, 821–832.

[9] Illingworth, Peter J., Christos Venetis, David K. Gardner, Scott M. Nelson, Jørgen Berntsen, Mark G. Larman, Franca Agresta et al. "Deep learning versus manual morphology-based embryo selection in IVF: a randomized, double-blind noninferiority trial." Nature Medicine 30, no. 11 (2024): 3114-3120.

[10] Boucret, Lisa, Floris Chabrun, Magalie Boguenet, Pascal Reynier, Pierre-Emmanuel Bouet, and Pascale May-Panloup. "Deep-learning model for embryo selection using time-lapse imaging of matched high-quality embryos." Scientific reports 15, no. 1 (2025): 28068.

[11] Huo, Wen-jie, Fei Peng, Song Quan, and Xiao-cong Wang. "Development and validation of machine learning models for predicting blastocyst yield in IVF cycles." Scientific Reports 15, no. 1 (2025): 22631.

[12] Canon, Chelsea, Lily Leibner, Michael Fanton, Zeyu Chang, Vaishali Suraj, Joseph A. Lee, Kevin Loewke, and David Hoffman. "Optimizing oocyte yield utilizing a machine learning model for dose and trigger decisions, a multi-center, prospective study." Scientific Reports 14, no. 1 (2024): 18721.

[13] Wang, Guangyu, Kai Wang, Yuanxu Gao, Longbin Chen, Tianrun Gao, Yuanlin Ma, Zeyu Jiang et al. "A generalized AI system for human embryo selection covering the entire IVF cycle via multi-modal contrastive learning." Patterns 5, no. 7 (2024).

[14] Ueno, Satoshi, Jørgen Berntsen, Tadashi Okimura, and Keiichi Kato. "Improved pregnancy prediction performance in an updated deep-learning embryo selection model: a retrospective independent validation study." Reproductive biomedicine online 48, no. 1 (2024): 103308.

[15] Sharma, Akriti, Alexandru Dorobantiu, Saquib Ali, Mario Iliceto, Mette H. Stensen, Erwan Delbarre, Michael A. Riegler, and Hugo L. Hammer. "Deep learning methods to forecasting human embryo development in time-lapse videos." PLoS One 20, no. 9 (2025): e0330924.

[16] Borna, Mahdi-Reza, Mohammad Mehdi Sepehri, and Behnam Maleki. "An artificial intelligence algorithm to select most viable embryos considering current process in IVF labs." Frontiers in artificial intelligence 7 (2024): 1375474.

[17] Kim, Young-Woo, Andreas Melzer, Susie Kim, and Paul Barach. "Promises and Perils of Artificial Intelligence in Surgery: The Critical Pathways for Successful Healthcare Outcomes." In Artificial Intelligence and the Perspective of Autonomous Surgery, pp. 99-118. Cham: Springer Nature Switzerland, 2024.

[18] Bhat, Ghulam Rasool, Farooz Ahmad Lone, and Jasmer Dalal. "Microfluidics—A novel technique for high-quality sperm selection for greater ART outcomes." FASEB BioAdvances 6, no. 10 (2024): 406-423.

[19] Yao, Mylene WM, Elizabeth T. Nguyen, Matthew G. Retzloff, L. April Gago, John E. Nichols, John F. Payne, Barry A. Ripps et al. "Machine learning center-specific models show improved IVF live birth predictions over US national registry-based model." Nature Communications 16, no. 1 (2025): 3661.

[20] Sergeev, Sergey A., Iuliia Diakova, and Veniamin Khazarinov. "Dissociating Ranking from Accuracy in Ivf: Image-Based Ai Enhances Embryo Prioritization Without Improving Predictive Performance." Available at SSRN 5385818(2025).

[21] Salih, Mohamed, Christopher Austin, Krishna Mantravadi, Eva Seow, Sutthipat Jitanantawittaya, Sandeep Reddy, Beverley Vollenhoven, Hamid Rezatofighi, and Fabrizzio Horta. "Deep learning classification integrating embryo images with associated clinical information from ART cycles." Scientific Reports 15, no. 1 (2025): 17585.

[22] Sawada, Yuki, Takeshi Sato, Masashi Nagaya, Chieko Saito, Hiroyuki Yoshihara, Chihiro Banno, Yosuke Matsumoto et al. "Evaluation of artificial intelligence using time-lapse images of IVF embryos to predict live birth." Reproductive biomedicine online 43, no. 5 (2021): 843-852.

[23] Berman, Aya, Roi Anteby, Orly Efros, Eyal Klang, and Shelly Soffer. "Deep learning for embryo evaluation using time-lapse: a systematic review of diagnostic test accuracy." American Journal of Obstetrics and Gynecology 229, no. 5 (2023): 490-501.

[24] Ouyang, Xueqiang, and Jia Wei. "Multi-Modal Artificial Intelligence of Embryo Grading and Pregnancy Prediction in Assisted Reproductive Technology: A Review." arXiv preprint arXiv:2505.20306 (2025).

[25] Sharma, Akriti, Alexandru Dorobantiu, Saquib Ali, Mario Iliceto, Mette H. Stensen, Erwan Delbarre, Michael A. Riegler, and Hugo L. Hammer. "Deep learning methods to forecasting human embryo development in time-lapse videos." PLoS One 20, no. 9 (2025): e0330924.

[26] Dehghan, Shirin, Reza Rabiei, Hamid Choobineh, Keivan Maghooli, Mozhdeh Nazari, and Mojtaba Vahidi-Asl. "Comparative study of machine learning approaches integrated with genetic algorithm for IVF success prediction." Plos one 19, no. 10 (2024): e0310829.

[27] Peng, Junwei, Xiaoyujie Geng, Yiyue Zhao, Zhijin Hou, Xin Tian, Xinyi Liu, Yuanyuan Xiao, and Yang Liu. "Machine learning algorithms in constructing prediction models for assisted reproductive technology (ART) related live birth outcomes." Scientific Reports 14, no. 1 (2024): 32083.

[28] Dalal, Rutvij Jay, and Akanksha P. Mishra. "Artificial intelligence in assisted reproductive technology: present and future." International Journal of Infertility & Fetal Medicine 11, no. 3 (2020): 61-64.

[29] Raimundo, J. M., and P. Cabrita. "Artificial intelligence at assisted reproductive technology." Procedia Computer Science 181 (2021): 442-447.

[30] Amini Mahabadi, Javad, Seyed Ehsan Enderami, Hossein Nikzad, and Hassan Hassani Bafrani. "The Use of Machine Learning for Human Sperm and Oocyte Selection and Success Rate in IVF Methods." Andrologia 2024, no. 1 (2024): 8165541.

[31] Hassan, Md Rafiul, Sadiq Al-Insaif, M. Imtiaz Hossain, and Joarder Kamruzzaman. "A machine learning approach for prediction of pregnancy outcome following IVF treatment." Neural computing and applications 32, no. 7 (2020): 2283-2297.

[32] Barnett-Itzhaki, Zohar, Miriam Elbaz, Rachely Butterman, Devora Amar, Moshe Amitay, Catherine Racowsky, Raoul Orvieto, Russ Hauser, Andrea A. Baccarelli, and Ronit Machtinger. "Machine learning vs. classic statistics for the prediction of IVF outcomes." Journal of assisted reproduction and genetics 37, no. 10 (2020): 2405-2412.

[33] Badr, Sanaa, Meryem Tahri, Mohamed Maanan, Jan Kašpar, and Noura Yousfi. "An intelligent decision-making system for embryo transfer in reproductive technology: a machine learning-based approach." Systems Biology in Reproductive Medicine 71, no. 1 (2025): 13-28.

[34] Isa, Iza Sazanita, Umi Kalsom Yusof, and Murizah Mohd Zain. "Image processing approach for grading IVF blastocyst: A state-of-the-art review and future perspective of deep learning-based models." Applied Sciences 13, no. 2 (2023): 1195.

[35] Srivastava, Diplav, Saumya Gupta, Srinivas Kudavelly, and Ramaraju Ga. "Unsupervised deep learning based longitudinal follicular growth tracking during IVF cycle using 3D transvaginal ultrasound in assisted reproduction." In 2021 43rd Annual International Conference of the IEEE Engineering in Medicine & Biology Society (EMBC), pp. 3209-3212. IEEE, 2021.

[36] Cohen, Jacques, Giuseppe Silvestri, Omar Paredes, Hector E. Martin-Alcala, Alejandro Chavez-Badiola, Mina Alikani, and Giles A. Palmer. "Artificial intelligence in assisted reproductive technology: separating the dream from reality." Reproductive BioMedicine Online 50, no. 4 (2025): 104855.

[37] Lee, Chun-I., Yan-Ru Su, Chien-Hong Chen, T. Arthur Chang, Esther En-Shu Kuo, Wei-Lin Zheng, Wen-Ting Hsieh, Chun-Chia Huang, Maw-Sheng Lee, and Mark Liu. "End-to-end deep learning for recognition of ploidy status using time-lapse videos." Journal of Assisted Reproduction and Genetics 38, no. 7 (2021): 1655-1663.

[38] Chen, Kuo, Jing Zuo, Wei Han, and Jin-hong Guo. "Review of intelligent methods for embryo health assessment in assisted reproductive technologies." LabMed Discovery (2025): 100075.